

Performance Improvement of A356 Cast Aluminum Alloy by Adding TiO₂ Powder and Stirring in Microstructure and Strength

Tiwan Tiwan^{1,2*}, Didik Nurhadiyanto^{1,2}, Mujiyono Mujiyono^{1,2}, Febrianto Amri Restadi^{1,2}

¹ Department of Mechanical Engineering Education, Faculty of Engineering, Universitas Negeri Yogyakarta, Jl. Colombo No. 1, 55281 Yogyakarta, Indonesia

² Center for Eco-Material Engineering and Manufacturing, Universitas Negeri Yogyakarta, Jl. Colombo No. 1, 55281 Yogyakarta, Indonesia

* Corresponding author, e-mail: tiwan@uny.ac.id

Received: 23 April 2025, Accepted: 11 June 2025, Published online: 30 June 2025

Abstract

This study aims to improve the performance of A356 cast aluminum alloy by incorporating titanium dioxide (TiO₂) powder and applying variations in stirring speed during processing. The effects of these modifications were evaluated based on microstructural characteristics, tensile strength, and impact strength. The methodology includes a casting process with TiO₂ concentrations of 0%, 5%, 10%, and 15% by weight, along with variations in stirring speed (300, 400, 500 and 600 RPM) to ensure homogeneous powder distribution within the aluminum matrix. The mechanical properties of the A356 + TiO₂ composite, including tensile strength, elastic modulus, strain, and impact energy, were evaluated. Furthermore, the material's microstructure was examined using optical microscopy. The results indicate that the addition of TiO₂ contributes to an increased titanium content in the alloy, leading to microstructural changes characterized by the formation of finer dendrites. Furthermore, the combination of TiO₂ addition and increased stirring speed significantly enhances the material's tensile and impact strength. With the addition of TiO₂ by 15%, there is an increase in tensile strength of 14.2% and impact strength of 21%. Likewise, with an increase in rotation up to 600 RPM, tensile strength increases by 14.9% and impact strength increases by 8.2%. These findings provide valuable insights into the development of advanced aluminum-based materials for industrial applications, particularly in the automotive and aerospace sectors.

Keywords

aluminum A356, TiO₂, strength, microstructure, stirring

1 Introduction

The A356 aluminum alloy has become one of the prominent materials in the automotive, aerospace, and electrical industries due to its combination of good mechanical properties, lightweight, and corrosion resistance [1, 2]. In these various applications, the enhancement of mechanical properties, such as tensile strength, has become an urgent need to support the performance of components in increasingly complex operational conditions. One way to improve the mechanical properties of this material is by utilizing composite material technology, which involves adding reinforcement particles into the aluminum matrix [3, 4].

Cast aluminum alloys can be reinforced with various types of particles to improve their mechanical properties [5–7]. Silicon carbide (SiC) and aluminum oxide (Al₂O₃) are commonly used ceramic particles due to their

high hardness and good thermal stability [8–10]. Carbon nanotubes (CNTs) and graphene from the carbon group offer advantages in tensile strength and thermal conductivity [11, 12]. Boride particles such as titanium diboride (TiB₂) and zirconium diboride (ZrB₂) are known for their high-temperature resistance and hardness [13, 14]. Fly ash is used as an economical, environmentally friendly reinforcement [15], while magnesium oxide (MgO) is suitable for applications in corrosive environments [16]. The combination of these particles with aluminum creates a tough, lightweight, and wear-resistant composite material for various technical applications [17, 18].

To improve the quality of cast aluminum, various methods, parameters, and processing treatments are employed [19, 20]. Stir casting is the most common method,

where reinforcing particles are mixed into molten aluminum using mechanical stirring [21–23]. Important parameters such as pouring temperature, stirring speed, and particle distribution must be controlled to ensure composite homogeneity. Heat treatments such as annealing or solution treatment are often performed to optimize the microstructure and improve the material's strength [24, 25]. Additionally, techniques like spray deposition can be used to produce composites with strong bonds between the aluminum matrix and reinforcing particles [26–28]. All of these steps aim to produce cast aluminum that is stronger, more wear-resistant, and possesses superior mechanical properties. Titanium dioxide (TiO_2) powder is one of the reinforcement materials with great potential to improve the mechanical properties of aluminum alloys [29]. With good strength and thermal stability characteristics, TiO_2 can significantly strengthen the aluminum matrix [30]. Moreover, the addition of this reinforcing powder can also affect the alloy's microstructure, such as phase distribution and grain size, which ultimately determines the mechanical properties of the material [31, 32].

The success of adding TiO_2 as a reinforcement in AA356 alloy depends not only on the concentration of the powder used but also on the process parameters during its production. One important parameter is the stirring speed during the mixing process. The right stirring speed can ensure homogeneous distribution of TiO_2 powder within the matrix, resulting in uniform microstructure and optimal mechanical properties [33]. On the other hand, improper stirring can lead to segregation, porosity, or other defects that reduce the material's performance [21, 34].

The relationship between variations in TiO_2 powder concentration and stirring speed on the mechanical properties and microstructure of AA356 is a relevant topic for further research. A deep understanding of these parameters' effects could provide new insights into the development of superior aluminum-based materials. Therefore, this research is expected to contribute significantly to improving the quality of aluminum alloy products for industrial applications. This study aims to improve the performance of A356 cast aluminum alloy by adding titanium dioxide (TiO_2) powder and varying the stirring speed on the microstructure, tensile strength and impact strength.

2 Materials and methods

2.1 Preparation

The main material used in this study is AA356 cast aluminum alloy, which was obtained in the form of ingots, along

with TiO_2 powder as the reinforcing material, as shown in Tables 1 and 2. The TiO_2 powder used is ROFA brand, with a purity of 99% and a crystal size of 15.554 nm. TiO_2 powder was added in varying concentrations of 0%, 5%, 10%, and 15% by weight to observe its effect on the mechanical properties and microstructure of the material.

2.2 Mixing and casting process

The process begins with the melting of AA356 aluminum alloy using a melting furnace at a temperature of approximately 700 °C until the aluminum reaches a fully molten state. Afterward, TiO_2 powder is added to the molten aluminum using the mechanical stirring method. The stirring speeds applied were 400 RPM, 500 RPM, and 600 RPM, maintained for a specific duration to ensure optimal mixing. Once the mixing process is complete, the molten aluminum is poured into a metal mold and allowed to solidify naturally. A depiction of the casting material preparation process can be seen in Fig. 1.

2.3 Material characterization

Tensile test specimens were prepared according to the ASTM E8/E8M-24 standard [35] for tensile strength testing. The dimensions of the tensile test specimens are shown in Fig. 2. The testing was carried out using a universal testing machine (UTM) to measure the maximum tensile strength of each sample variation. Fig. 3 illustrates the specimen for impact testing based on ASTM E23-25 standard [36]. A total of 24 specimens were utilized for each of the tensile and impact tests, with three replicates conducted for each experimental condition. Additionally, microstructure analysis was performed using an optical microscope (OM) to observe the distribution, grain size, and the presence of other phases formed due to the addition of reinforcement.

The tensile strength test results were analyzed to determine the effect of varying TiO_2 concentrations and stirring speeds on the improvement of the material's tensile strength. The microstructure was analyzed to evaluate the

Table 1 Composition of A356 aluminum

Al	Si	Mg	Cu	Mn	Fe	Ti	Zn
91.87	6.53	0.37	0.12	0.12	0.34	0.10	0.35

Table 2 Composition of titanium dioxide (TiO_2)

Element	TiO_2
Brand	ROFA
%	≥98

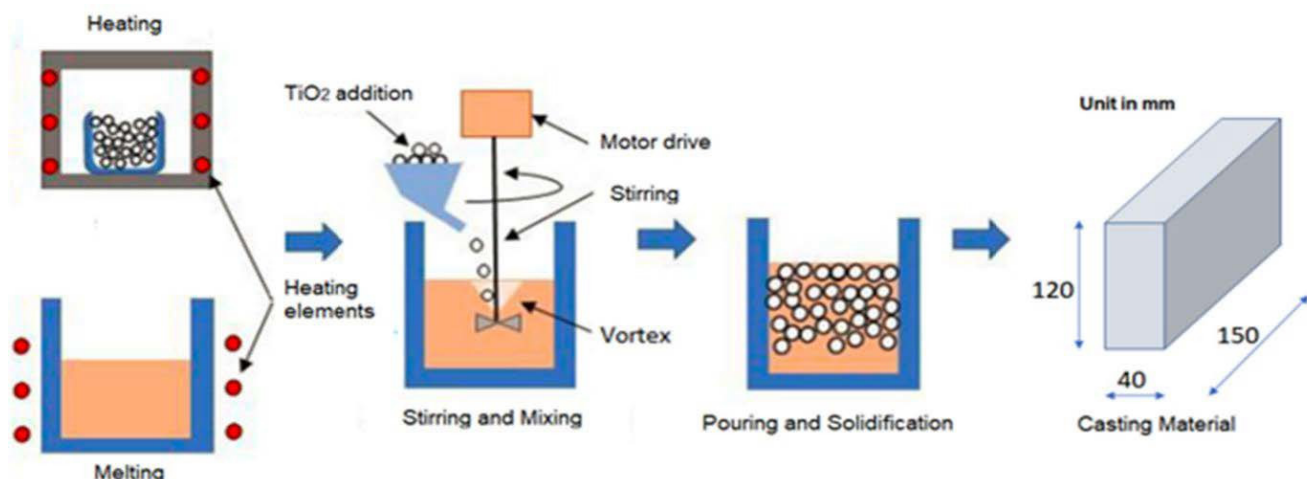


Fig. 1 Preparation process of modified casting material A356 plus TiO_2

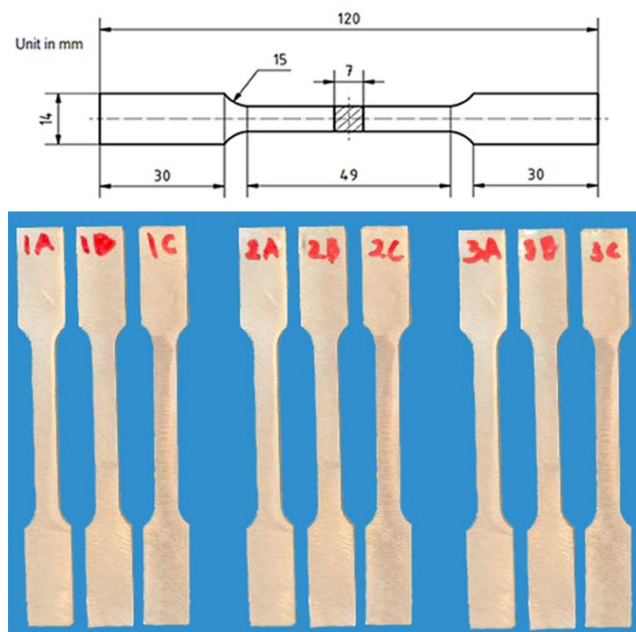


Fig. 2 Tensile test specimen (unit in mm)

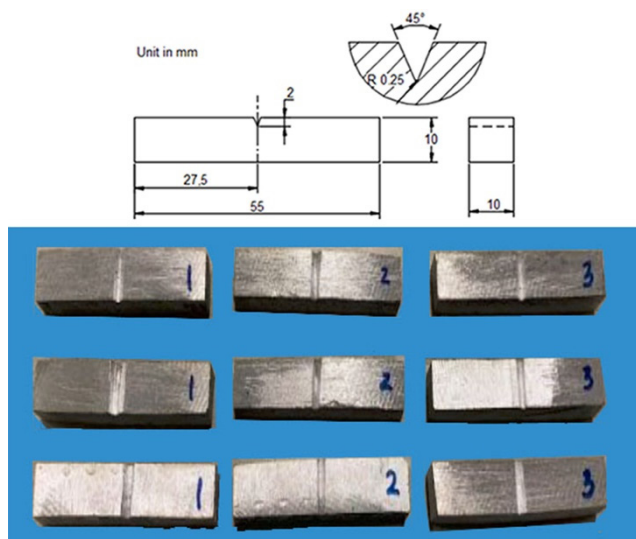


Fig. 3 Impact test specimen

uniformity of TiO_2 particle distribution and its impact on the material properties. Statistical analysis was performed to identify the relationship between the process parameters and the test results using data analysis.

3 Results and discussion

3.1 Composition of A356 + TiO_2

The proportion of elements present in a material can influence its physical and mechanical properties, such as strength, hardness, ductility, and toughness. Table 3 presents the results of the chemical composition test for aluminum A356 in its raw material condition and with varying additions of titanium dioxide.

Based on the data in Table 3, there is a difference in the chemical composition test results before and after the melting process of aluminum A356. The mixing of aluminum A356 before and after melting causes changes in the composition of each chemical element in the metal. This change in composition can occur when titanium dioxide is added during the casting process. This is due to the fact that the melting process involves the liquefaction, diffusion, and mixing of different metals.

3.2 Microstructure

Fig. 4 shows a visual representation of the microstructure of the raw material A356 and the alloy that has been added with TiO_2 powder. The microstructure of A356 in its raw material form (Fig. 4 (a)) appears relatively brighter with a sparser dendritic structure. This affects the mechanical properties of the material, which are lower compared to the material with added titanium dioxide. The raw material aluminum A356 has an average dendritic grain size of $167.69 \mu\text{m}^2$.

The microstructure of aluminum A356 with the addition of TiO_2 shows significant changes in the form

Table 3 Results of A356 + TiO₂ casting composition test

Material cast	Elements (% weight)							
	Al	Si	Mg	Zn	Cu	Mn	Ti	Ni
Raw A356	91.872	6.531	0.374	0.353	0.129	0.127	0.101	0.004
A356 + 5% TiO ₂	91.794	6.553	0.341	0.368	0.132	0.126	0.102	0.005
A356 + 10% TiO ₂	91.829	6.309	0.337	0.370	0.136	0.129	0.103	0.004
A356 + 15% TiO ₂	91.813	6.411	0.333	0.339	0.126	0.129	0.106	0.005

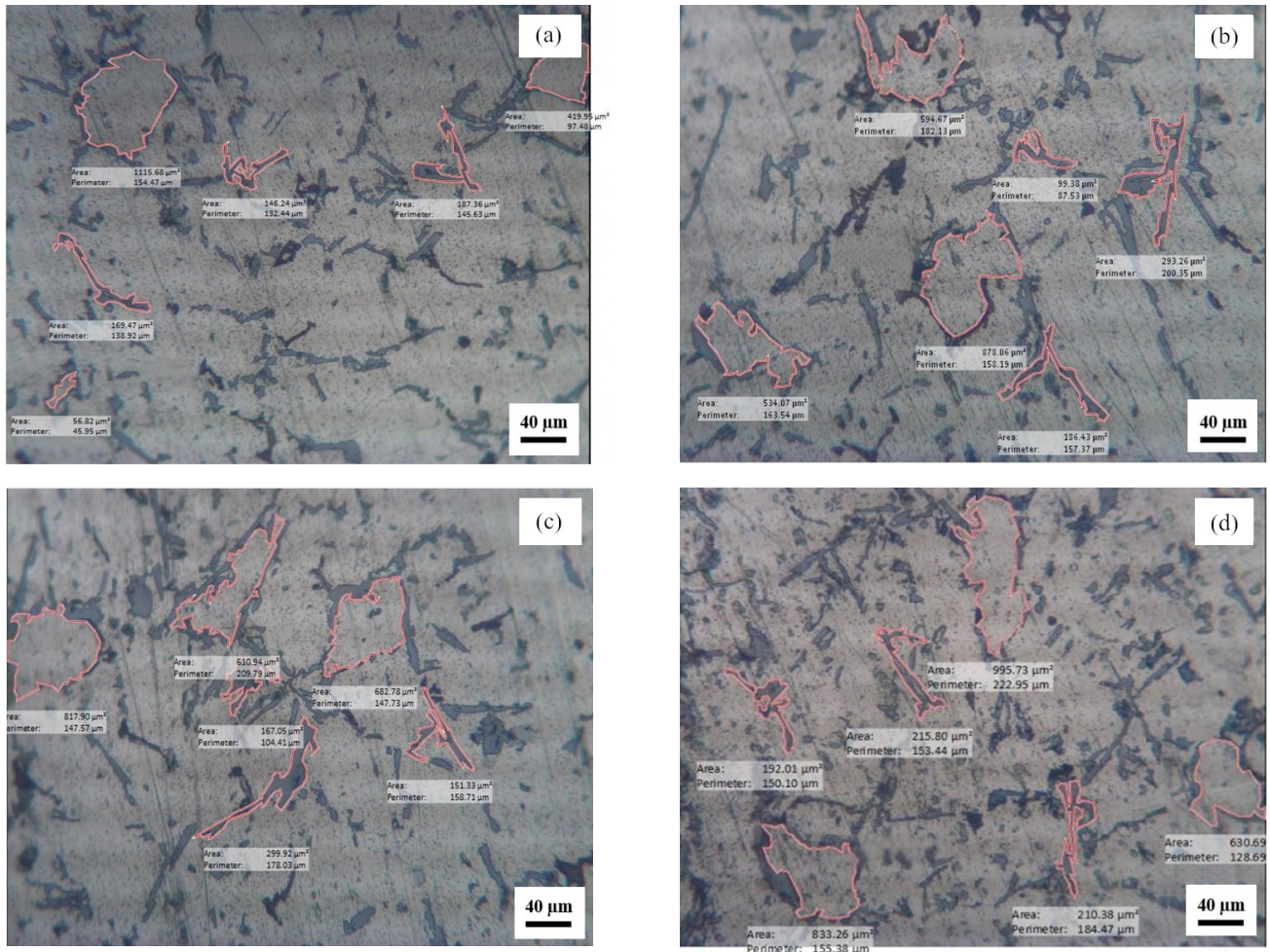


Fig. 4 Microstructure of A356 cast aluminum alloy (a) raw material, (b) +5% TiO₂, (c) +10% TiO₂ and (d) +15% TiO₂

and distribution of dendrites. In the 5% TiO₂ variation (Fig. 4 (b)), the dendritic structure appears more compact with longer arms, which is caused by the accelerated solidification due to the presence of TiO₂. The average dendrite size in this variation reaches 193.02 μm².

In the 10% TiO₂ variation (Fig. 4 (c)), the dendritic structure undergoes further changes, with longer and wider arms compared to the previous variation, resulting in an increase in the average dendrite size to 206.1 μm². This change contributes to the improvement in tensile strength and hardness of the material due to the formation of more precipitates, which act as additional nucleation sites for solidification [37].

In the 15% TiO₂ variation (Fig. 4 (d)), the dendritic structure becomes even denser with a higher number of dendrites, caused by a higher rate of solidification compared to the other variations. Chemical composition analysis shows that the higher the amount of TiO₂ added, the greater the Ti content in the alloy, which directly affects the microstructure. The average dendrite size in this variation is 259.95 μm², showing the most significant effect in microstructure changes. Thus, the increase in TiO₂ concentration leads to an enhancement in the microstructure, contributing to the improvement of the mechanical properties of aluminum A356 [38].

The effect of stirring speed on the microstructure of A356 aluminum alloy with the addition of 15% TiO_2 shows significant changes in grain size and its distribution as seen in Fig. 5. At a stirring speed of 400 RPM (Fig. 5 (a)),

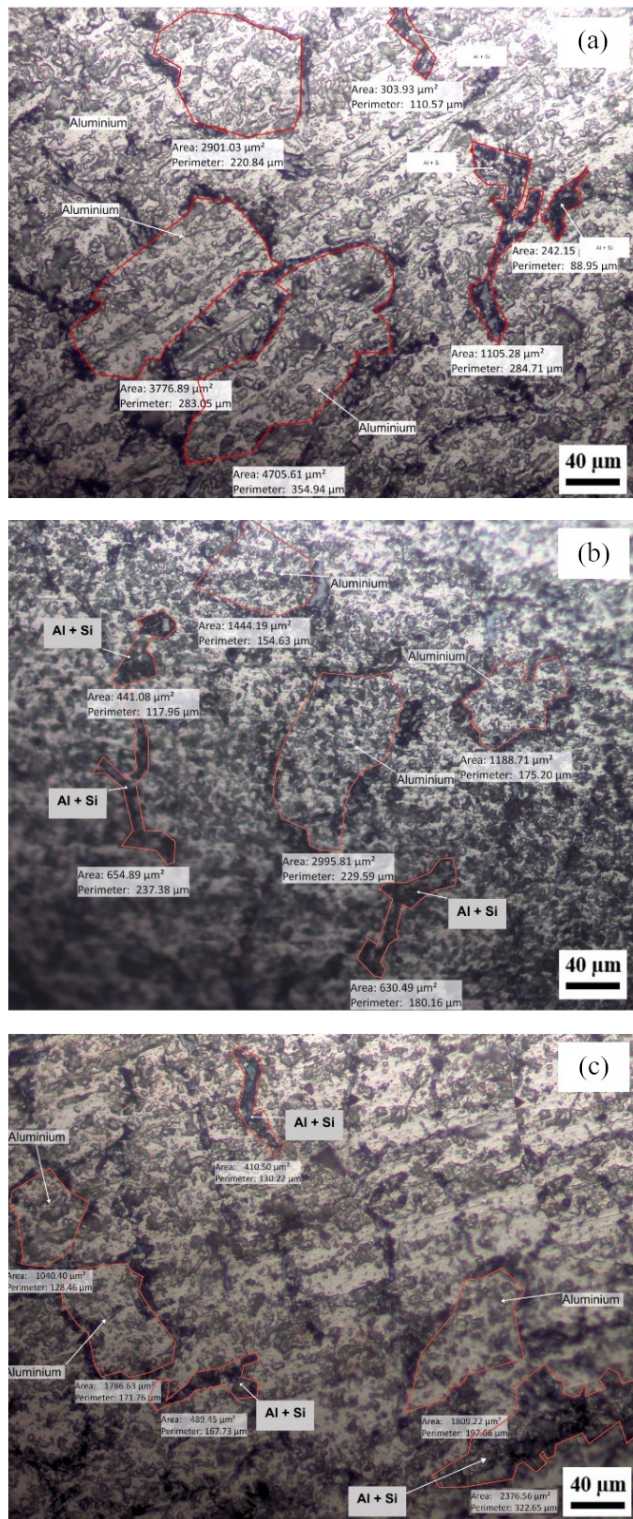


Fig. 5 Microstructure of aluminum A356 + 15% TiO_2 with variations in stirring speed: (a) 400 rpm, (b) 500 rpm and (c) 600 rpm

the microstructure shows the initial formation of dendrites with long arms. This indicates that the increased stirring speed begins to influence the growth of the micrograins, causing their size to gradually decrease. At this speed, the average aluminum grain size was recorded as $3794.51 \mu\text{m}^2$, while the average size of the Al + Si grain boundary was $550.45 \mu\text{m}^2$.

When the stirring speed was increased to 500 RPM (Fig. 5 (b)), the number and density of the dendrites increased, indicating more controlled grain growth. As a result, the aluminum grain size further decreased, with an average of $1915.51 \mu\text{m}^2$, while the average size of the Al + Si grain boundary dropped to $106.48 \mu\text{m}^2$. This more uniform microstructure contributes to an improvement in the material's strength.

At a stirring speed of 600 RPM (Fig. 5 (c)), the number of dendrites increased and became more compact compared to the previous stirring speed variations. The higher density and finer microstructure resulted in an increase in the elastic modulus, as well as the stress and strain values during tensile testing. At this speed, the average aluminum grain size reduced to $1545.42 \mu\text{m}^2$, while the average size of the Al + Si grain boundary significantly increased to $1092.17 \mu\text{m}^2$. From these results, it can be concluded that as the stirring speed increases, the micrograin size becomes smaller and the dendritic structure becomes denser, directly impacting the improvement of the material's mechanical properties [39].

3.3 Tensile test

Tensile testing was conducted to determine the mechanical properties, including maximum stress, strain, and elastic modulus (Young's modulus). Based on the graph showing the tensile test results for stress, strain, and elastic modulus in A356 aluminum with various TiO_2 addition variations, the tensile stress graph is presented in Fig. 6.

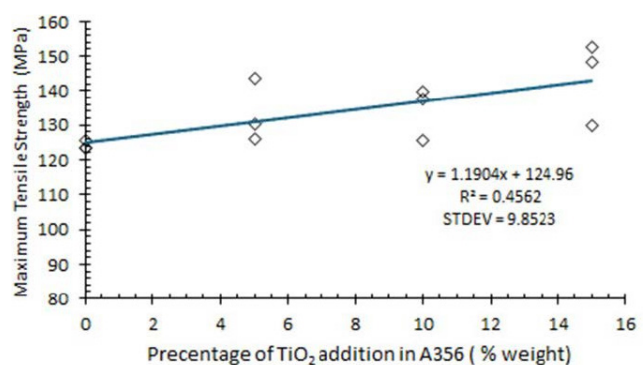


Fig. 6 Graph of tensile stress values of TiO_2 material variations

The test results indicate that A356 aluminum without TiO_2 exhibits the lowest tensile strength (124.136 MPa), primarily due to the dominance of coarse grains in its microstructure. The addition of 5% TiO_2 increases the tensile strength to 133.4 MPa as a result of dendrite arm elongation, grain size refinement, and enhanced grain boundaries, which contribute to material strengthening. With 10% TiO_2 , the tensile strength slightly rises to 134.36 MPa due to the formation of more solidification nuclei, which improves mechanical properties through enhanced grain boundary strengthening. The addition of 15% TiO_2 yields the highest tensile strength (143.65 MPa), attributed to the formation of finer grains and a denser dendritic structure, which increases resistance to dislocation movement and significantly enhances the material's strength. Therefore, the addition of 15% TiO_2 is considered as the optimal choice to improve the tensile strength of A356 aluminum with an average tensile strength increase of 14.2%.

The graph illustrating the strain values of A356 cast aluminum with and without varying additions of TiO_2 powder is shown in Fig. 7. The test results indicate that A356 aluminum without TiO_2 exhibits the lowest strain (3.7184%) due to the presence of relatively large microstructural grains. The addition of 5% TiO_2 increases the strain to 4.1451%, attributed to finer grains and elongated dendritic structures, which reduce grain size and enhance grain boundaries. With a 10% TiO_2 addition, the strain rises to 4.4024% due to a coarser dendritic structure that increases the number of grain boundaries and inhibits dislocation movement. The highest strain (4.9082%) is achieved with 15% TiO_2 , resulting from a finer microstructure, denser dendrites, and faster solidification, all of which enhance grain boundaries and more effectively hinder dislocation motion. Therefore, the 15% TiO_2 variation provides the most significant improvement in strain, making it the optimal choice for enhancing material deformability.

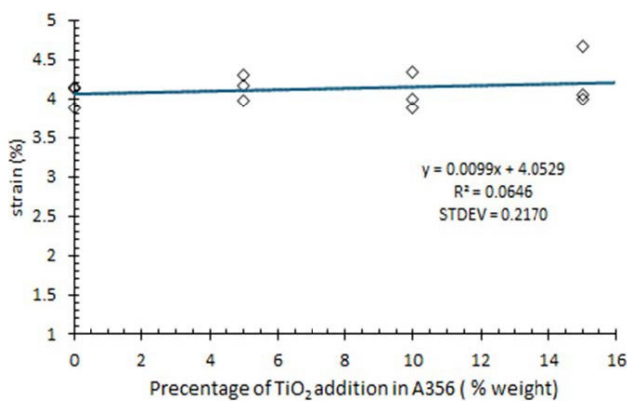


Fig. 7 Graph of strain value of material variation of TiO_2 addition

Fig. 8 presents the graph of the elastic modulus of A356 cast aluminum with and without the addition of TiO_2 powder. The test results show that A356 aluminum without TiO_2 has an elastic modulus of 5111.26 MPa, serving as the baseline reference for material stiffness. The addition of 5% TiO_2 results in a 9.2% decrease in elastic modulus to 4642.3 MPa, due to uneven particle distribution, although it contributes to improved ductility. With a 10% TiO_2 addition, the elastic modulus significantly increases to 7869.06 MPa, attributed to better particle distribution, which enhances dispersion strengthening and material stiffness. The highest elastic modulus (12993.6 MPa) is achieved with the addition of 15% TiO_2 , where uniform particle distribution provides maximum reinforcement and improves resistance to plastic deformation. Therefore, the greater the TiO_2 content, the higher the strength and stiffness of A356 aluminum [39].

A graph displaying the tensile strength test results of A356 aluminum alloy with 15% TiO_2 under different stirring speeds has been generated, as shown in Fig. 9. Tensile testing results of A356 aluminum with 15% TiO_2 show a progressive increase in tensile strength as the stirring speed increases. At 400 RPM, the average tensile strength rises to 145.29 N/mm² due to the formation of finer microstructural grains. At 500 RPM, the strength further increases to 146.25 N/mm², attributed to a higher number

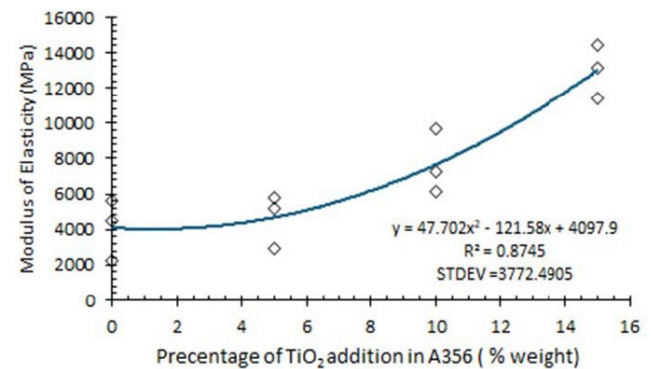


Fig. 8 Elasticity modulus graph of variation of TiO_2 addition

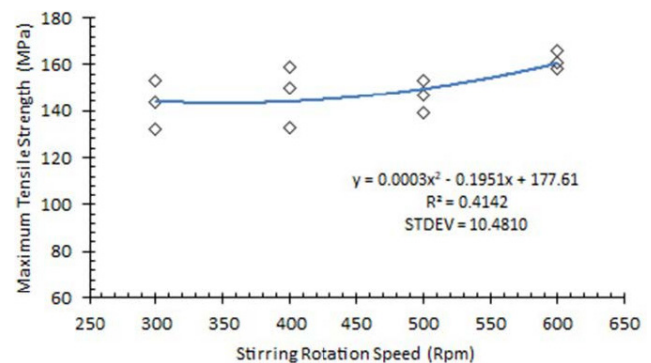


Fig. 9 Graph of tensile stress values of materials variation of stirring speed

of dendrites and a more refined microstructure. The highest tensile strength is observed at 600 RPM, reaching 161.67 N/mm^2 , resulting from the finest grain distribution and more uniform grain boundaries. Overall, increasing the stirring speed up to 600 RPM enhances the average tensile strength by 14.9%, making it the optimal condition for improving the tensile properties of A356 aluminum.

Strain test results also reveal the effect of stirring speed on deformation behavior, as shown in Fig. 10. At 400 RPM, the average maximum strain reaches 3.6780%, with the microstructure still dominated by coarse grains, resulting in a stiffer material where elastic deformation remains predominant. At 500 RPM, the strain slightly decreases to 3.4522%, indicating the material remains relatively rigid, with microstructural features not significantly different from those at 400 RPM. However, at 600 RPM, the strain increases significantly to 4.4748%, due to improved microstructure with finer grains and more uniform grain boundaries—signaling the onset of permanent deformation. Thus, a stirring speed of 600 RPM results in the highest strain, consistent with the observed increase in tensile strength.

Fig. 11 presents the elastic modulus of the material A356 aluminum composed of 15% TiO_2 under varying stirring speeds. At 400 RPM, the average elastic modulus

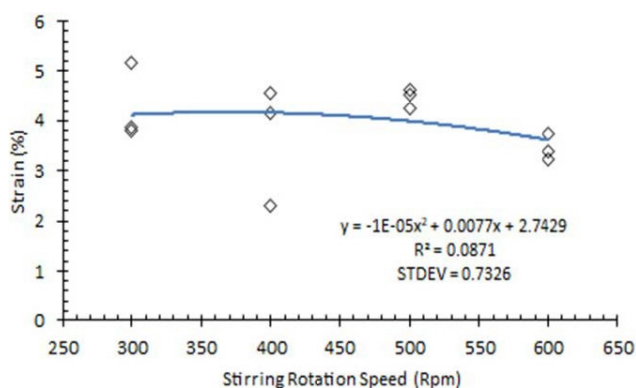


Fig. 10 Graph of material strain values for stirring speed variations

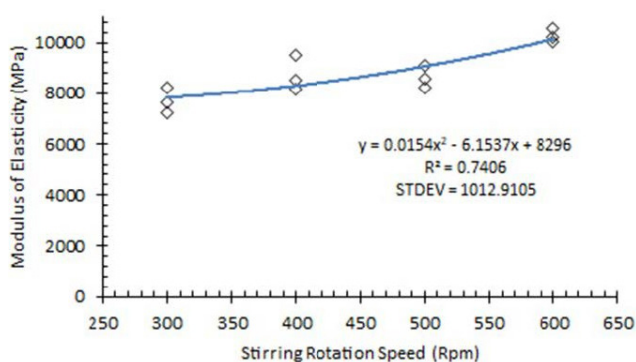


Fig. 11 Graph of elastic modulus of stirring speed variation

reaches 7690.2 N/mm^2 , indicating increased stiffness due to microstructural reorientation and the influence of centrifugal forces. At 500 RPM, a slight decrease is observed, with the modulus dropping to 9690.6 N/mm^2 , likely caused by dispersion failure and weakened atomic bonding, although the material still adapts to applied loads. At 600 RPM, the elastic modulus increases significantly to $10,277.7 \text{ N/mm}^2$, reflecting a more organized microstructure that is optimally resistant to applied stress. Therefore, a stirring speed of 600 RPM results in the highest elastic modulus, indicating a maximum improvement in material stiffness.

3.4 Impact test

Charpy impact tests were conducted on three test specimens for each variation of titanium dioxide addition to ensure the reliability and convergence of the data obtained. The tests utilized a small pendulum capable of absorbing a maximum energy of 150 J. The graph displaying the Charpy impact test results for A356 aluminum with various TiO_2 additions is shown in Fig. 12.

The impact test results show that A356 aluminum without TiO_2 exhibits the lowest toughness (0.042 J/mm^2), due to a microstructure dominated by coarse grains and loosely packed dendrites, leading to brittle fracture with a coarse granular pattern. The addition of 5% TiO_2 increases the toughness to 0.0443 J/mm^2 , attributed to longer and more tightly packed dendrites that improve energy distribution during impact. With 10% TiO_2 , toughness further increases to 0.0476 J/mm^2 , as the growth of larger dendrites enhances the material's energy absorption capability, although the fracture behavior remains predominantly brittle.

The highest toughness value (0.0506 J/mm^2) is achieved with the addition of 15% TiO_2 , resulting from finer grains and increasingly compact dendritic structures that improve

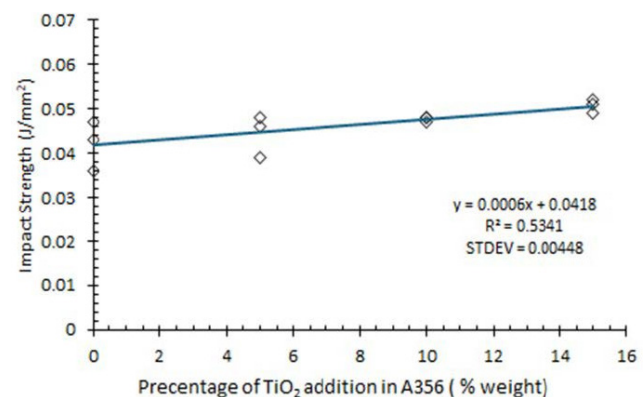


Fig. 12 Charpy impact toughness value graph of variation of TiO_2 addition

stress distribution and resistance to impact. Although the fracture mode remains brittle, the fracture surface appears smoother, displaying a granular pattern resembling fine crystals. Overall, increasing TiO_2 concentration directly enhances the toughness of A356 aluminum, with 15% of TiO_2 identified as the optimal variation for maximizing impact energy absorption increasing by 21%.

The graph of Charpy impact toughness for A356 aluminum with a 15% TiO_2 addition at various stirring speeds is presented in Fig. 13.

Impact test results indicate that at a stirring speed of 400 RPM, the average toughness reaches 0.054 J/mm^2 , attributed to the effects of strain hardening and grain redistribution within the microstructure, which enhance the material's ability to absorb impact energy. This improvement aligns with tensile test results that show increases in both elastic modulus and Brinell hardness. At 500 RPM, toughness further increases to 0.055 J/mm^2 due to a more uniform grain distribution within the microstructure, which strengthens the material's resistance to impact.

The highest toughness is achieved at a stirring speed of 600 RPM, with an average value of 0.057 J/mm^2 . At this speed, an average toughness increase of 8.2% occurred. The microstructure under this condition features finer grains and more uniform grain boundaries, improving material homogeneity and resistance to crack propagation. Additionally, the increasingly uniform distribution of TiO_2 particles contributes to enhanced toughness. Therefore, higher stirring speeds during the casting process lead to greater impact toughness, with 600 RPM identified as the optimal condition for improving the impact resistance of A356 aluminum [40].

In accordance with the Hall–Petch relationship, the strength of a material is inversely proportional to its grain size [41]:

$$\sigma_y = \sigma_i + k_y d^{-\frac{1}{2}} \quad (1)$$

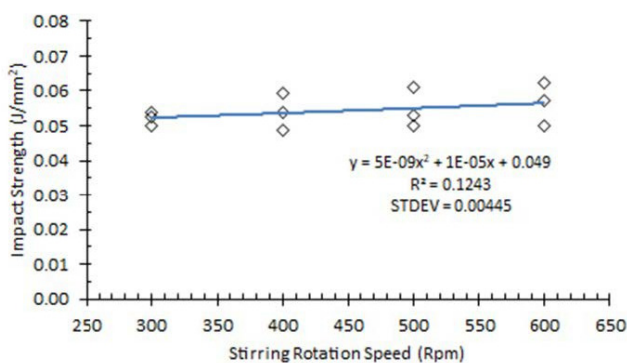


Fig. 13 Charpy impact toughness value graph of stirring speed variation

where d is the average grain diameter, σ_i and k_y are constants specific to the metal. A reduction in grain size leads to an increase in material strength. The strength of A356 increases as the addition of TiO_2 and the stirring speed are increased, both of which contribute to grain refinement. The resulting finer grain structure enhances the overall strength of the material.

In addition to grain refinement, the increase in strength is also attributed to precipitation strengthening by TiO_2 , as explained by the Orowan mechanism [42]. The addition of TiO_2 leads to the formation of precipitates within the grains, and their distribution becomes more uniform with the aid of stirring. These intragranular precipitates impede dislocation motion, thereby increasing the material's resistance to deformation. When an external load is applied, dislocations move and approach the aligned precipitates due to the acting stress. As dislocations continue to move, they are obstructed by the precipitates. Since the precipitates are sufficiently strong, dislocations are unable to shear through them. This hindrance to dislocation movement results in precipitation strengthening. This phenomenon explains why the combination of 15% TiO_2 addition and a stirring speed of 600 RPM yields the highest strength in the material. The results indicate that the A356 aluminum alloy reinforced with TiO_2 exhibits favorable strength and toughness. These properties make it a promising candidate for use in various automotive and aerospace applications. In the automotive sector, A356 is commonly utilized in components such as engine blocks, cylinder heads, and wheels, contributing to the development of lighter and stronger vehicles. In aerospace applications, the alloy's low density and excellent corrosion resistance are particularly advantageous, with typical uses including landing gear, wing structures, and fuselage frames, all of which contribute to reducing the overall weight of the aircraft [43].

4 Conclusion

The mechanical properties of A356 aluminum alloy can be effectively modified through the addition of TiO_2 powder and the application of stirring during the melting process. Structural transformations and enhancements in mechanical performance were observed as a result of these treatments, with the following key findings:

- The chemical composition of A356 is altered with the addition of TiO_2 powder, where the titanium content tends to increase proportionally with the amount of TiO_2 introduced.

- Significant microstructural changes occur with the addition of TiO_2 and the implementation of stirring. An increase in both TiO_2 content and stirring speed promotes the formation of finer dendritic structures within the alloy.
- The tensile and impact strength of A356 castings improves with higher TiO_2 additions and increased stirring speeds, indicating a direct correlation between processing conditions and mechanical performance enhancement. The addition of 15% TiO_2

increases the tensile strength by 14.2% and the impact strength by 21%. While the increase in stirring speed to 600 RPM increases the tensile strength by 14.9% and the impact strength by 8.2%.

Acknowledgement

The authors would like to express their gratitude to the Ministry of Research, Technology, and Higher Education of the Republic Indonesia for providing funding support for this research in Project no. T/56.22/UN34.15/PT.01.02/2024.

References

- [1] Kridli, G. T., Friedman, P. A., Boileau, J. M. "Chapter 7 - Manufacturing processes for light alloys", In: Mallick, P. K. (ed.) *Materials, Design and Manufacturing for Lightweight Vehicles* (Second Edition), Woodhead Publishing, 2021, pp. 267–320. ISBN 978-0-12-818712-8 <https://doi.org/10.1016/B978-0-12-818712-8.00007-0>
- [2] Kovács, J., Lukács, J. "Investigation of the Possibility for Compensating the HAZ Softening of AA7075-T6", *Periodica Polytechnica Mechanical Engineering*, 66(3), pp. 207–212, 2022. <https://doi.org/10.3311/PPme.19033>
- [3] de Damborenea, J., Conde, A., Gardon, M., Ravi, G. A., Arenas, M. A. "Effect of growth orientation and heat treatment on the corrosion properties of AISi10Mg alloy produced by additive manufacturing", *Journal of Materials Research and Technology*, 18, pp. 5325–5336, 2022. <https://doi.org/10.1016/j.jmrt.2022.05.021>
- [4] Sigdel, S., Dalal, P., Sanchaniya, S., Rachchh, N., Trivedi, D. "Mechanical and Thermal Characterization of Graphene and TiO_2 -Reinforced 4032 Aluminum Alloy for Piston Applications Using Mean Field Homogenization", *Periodica Polytechnica Mechanical Engineering*, 69(1), pp. 32–39, 2025. <https://doi.org/10.3311/PPme.38391>
- [5] Bhowmik, A., Kumar, R., Beemkumar, N., Kumar, A. V., Singh, G., Kulshreshta, A., Mann, V. S., Santhosh, A. J. "Casting of particle reinforced metal matrix composite by liquid state fabrication method: A review", *Results in Engineering*, 24, 103152, 2024. <https://doi.org/10.1016/j.rineng.2024.103152>
- [6] Kareem, S. A., Anaele, J. U., Aikulola, E. O., Adewole, T. A., Bodunrin, M. O., Alaneme, K. K. "Design and selection of metal matrix composites reinforced with high entropy alloys – Functionality appraisal and applicability in service: A critical review", *Journal of Alloys and Metallurgical Systems*, 5, 100057, 2024. <https://doi.org/10.1016/j.jalmes.2024.100057>
- [7] Edoziuno, F. O., Akaluzia, R. O., Odoni, B. U., Edibo, S. "Experimental study on tribological (dry sliding wear) behaviour of polyester matrix hybrid composite reinforced with particulate wood charcoal and periwinkle shell", *Journal of King Saud University - Engineering Sciences*, 33(5), pp. 318–331, 2021. <https://doi.org/10.1016/j.jksues.2020.05.007>
- [8] Singh, B., Kumar, I., Saxena, K. K., Mohammed, K. A., Ijaz Khan, M., Ben Moussa, S., Shukhratovich Abdullaev, S. "A future prospects and current scenario of aluminium metal matrix composites characteristics", *Alexandria Engineering Journal*, 76, pp. 1–17, 2023. <https://doi.org/10.1016/j.aej.2023.06.028>
- [9] Ponhan, K., Weston, D., Tassenberg, K. "Influence of SiC nanoparticle contents on microstructural evolution and mechanical behavior of AZ91D magnesium matrix composites synthesised through a combination of a master pellet feeding technique and stir casting assisted by ultrasonic vibration", *Materials Today Communications*, 36, 106785, 2023. <https://doi.org/10.1016/j.mtcomm.2023.106785>
- [10] Dinesh Kumar, P. K., Darius Gnanaraj, S. "Studies on Al-Si based hybrid aluminium metal matrix nanocomposites", *Materials Today Communications*, 38, 108132, 2024. <https://doi.org/10.1016/j.mtcomm.2024.108132>
- [11] Rahman Hafeezur, A., Sundeep, D., Sastry, C. C., Krishnaiah, J., K Varadharaj, E. "Investigation of ballistic and mechanical properties of AINPB metal matrix composites reinforced with TiCN decorated graphene nano flakes for light armored vehicles", *Journal of Alloys and Compounds*, 992, 174482, 2024. <https://doi.org/10.1016/j.jallcom.2024.174482>
- [12] Sadhu, K. K., Mandal, N., Sahoo, R. R. "SiC/graphene reinforced aluminum metal matrix composites prepared by powder metallurgy: A review", *Journal of Manufacturing Processes*, 91, pp. 10–43, 2023. <https://doi.org/10.1016/j.jmapro.2023.02.026>
- [13] Singh, V., Murtaza, Q., Niranjan, M. S. "Analyzing the synergistic effects of hard ceramic TiB_2 and rare earth oxide La_2O_3 on mechanical behaviour, wear resistance, and residual stress of AA6061-T6 hybrid composite fabricated via ultrasonic-assisted stir casting", *Materials Chemistry and Physics*, 325, 129727, 2024. <https://doi.org/10.1016/j.matchemphys.2024.129727>
- [14] Karbalaee Akbari, M., Baharvandi, H. R., Shirvanimoghaddam, K. "Tensile and fracture behavior of nano/micro TiB_2 particle reinforced casting A356 aluminum alloy composites", *Materials and Design*, 66, pp. 150–161, 2015. <https://doi.org/10.1016/j.matdes.2014.10.048>
- [15] Vinoth Babu, N., Siva, M., Subramanian, M., Elakkiyadasan, R., Manoj Kumar, P. "Investigation of mechanical characteristics of SiC and flyash particle reinforced aluminium matrix composites", *Materials Today: Proceedings*, 62, pp. 4316–4321, 2022. <https://doi.org/10.1016/j.matpr.2022.04.829>
- [16] Thakur, A., Bandhu, D., Peshwe, D. R., Mahajan, Y. Y., Saxena, K. K., Eldin, S. M. "Appearance of reinforcement, interfacial product, heterogeneous nucleant and grain refiner of MgAl_2O_4 in aluminium metal matrix composites", *Journal of Materials Research and Technology*, 26, pp. 267–302, 2023. <https://doi.org/10.1016/j.jmrt.2023.07.121>

- [17] Omoniyi, P., Adekunle, A., Ibitoye, S., Olorunpomi, O., Abolusoro, O. "Mechanical and microstructural evaluation of aluminium matrix composite reinforced with wood particles", *Journal of King Saud University - Engineering Sciences*, 34(6), pp. 445–450, 2022. <https://doi.org/10.1016/j.jksues.2021.01.006>
- [18] Alaneme, K. K., Bodunrin, M. O., Okotete, E. A. "On the nano-mechanical properties and local strain rate sensitivity of selected Aluminium-based composites reinforced with metallic and ceramic particles", *Journal of King Saud University - Engineering Sciences*, 35(1), pp. 62–68, 2023. <https://doi.org/10.1016/j.jksues.2021.02.011>
- [19] Saini, D. K., Jha, P. K. "Fabrication of aluminum metal matrix composite through continuous casting route: A review and future directions", *Journal of Manufacturing Processes*, 96, pp. 138–160, 2023. <https://doi.org/10.1016/j.jmapro.2023.04.041>
- [20] Varga, D., Szlancsik, A. "Investigation of the Effect of Heat Treatment Time in Case of Recrystallization of Al99.5", *Periodica Polytechnica Mechanical Engineering*, 67(3), pp. 252–258, 2023. <https://doi.org/10.3311/PPme.22823>
- [21] Shinde, S. S., Barve, S. B. "Advances in hybrid aluminium metal matrix composite produced by stir casting route: A review on applications and fabrication characteristics", *Materials Today: Proceedings*, 2024. <https://doi.org/10.1016/j.matpr.2024.05.029>
- [22] Pandian, V., Kannan, S. "Processing and preparation of aerospace-grade aluminium hybrid metal matrix composite in a modified stir casting furnace integrated with mechanical super-sonic vibration squeeze infiltration method", *Materials Today Communications*, 26, 101732, 2021. <https://doi.org/10.1016/j.mtcomm.2020.101732>
- [23] Ramanathan, A., Krishnan, P. K., Muraliraja, R. "A review on the production of metal matrix composites through stir casting – Furnace design, properties, challenges, and research opportunities", *Journal of Manufacturing Processes*, 42, pp. 213–245, 2019. <https://doi.org/10.1016/j.jmapro.2019.04.017>
- [24] Gecu, R., Acar, S., Kisasoz, A., Altug Guler, K., Karaaslan, A. "Influence of T6 heat treatment on A356 and A380 aluminium alloys manufactured by thixoforging combined with low superheat casting", *Transactions of Nonferrous Metals Society of China*, 28(3), pp. 385–392, 2018. [https://doi.org/10.1016/S1003-6326\(18\)64672-2](https://doi.org/10.1016/S1003-6326(18)64672-2)
- [25] Kumar, P., Sharma, S., Chandra Kandpal, B. "Synthesis and mechanical characterization of biomass fly ash strengthened aluminium matrix composites", *Materials Today: Proceedings*, 26, pp. 266–272, 2020. <https://doi.org/10.1016/j.matpr.2019.11.236>
- [26] Bakshi, S. R., Wang, D., Price, T., Zhang, D., Keshri, A. K., Chen, Y., McCartney, D. G., Shipway, P. H., Agarwal, A. "Microstructure and wear properties of aluminum/aluminum-silicon composite coatings prepared by cold spraying", *Surface and Coatings Technology*, 204(4), pp. 503–510, 2009. <https://doi.org/10.1016/j.surfcoat.2009.08.018>
- [27] Pandey, V., Seetharam, R., Chelladurai, H. "A comprehensive review: Discussed the effect of high-entropy alloys as reinforcement on metal matrix composite properties, fabrication techniques, and applications", *Journal of Alloys and Compounds*, 1002, 175095, 2024. <https://doi.org/10.1016/j.jallcom.2024.175095>
- [28] Nassar, A. E., Nassar, E. E. "Properties of aluminum matrix Nano composites prepared by powder metallurgy processing", *Journal of King Saud University - Engineering Sciences*, 29(3), pp. 295–299, 2017. <https://doi.org/10.1016/j.jksues.2015.11.001>
- [29] Karbalaee Akbari, M., Shirvanimoghaddam, K., Hai, Z., Zhuiykov, S., Khayyam, H. "Nano TiB₂ and TiO₂ reinforced composites: A comparative investigation on strengthening mechanisms and predicting mechanical properties via neural network modeling", *Ceramics International*, 43(18), pp. 16799–16810, 2017. <https://doi.org/10.1016/j.ceramint.2017.09.077>
- [30] Vasava, A., Singh, D. "Development of hybrid surface composite of AA7075-T651 using TiO₂ and graphene through friction stir processing", *Materials Today: Proceedings*, 2023. <https://doi.org/10.1016/j.matpr.2023.04.668>
- [31] Karbalaee Akbari, M., Baharvandi, H. R., Mirzaee, O. "Nano-sized aluminum oxide reinforced commercial casting A356 alloy matrix: Evaluation of hardness, wear resistance and compressive strength focusing on particle distribution in aluminum matrix", *Composites Part B: Engineering*, 52, pp. 262–268, 2013. <https://doi.org/10.1016/j.compositesb.2013.04.038>
- [32] Mazahery, A., Shabani, M. O. "Plasticity and microstructure of A356 matrix nano composites", *Journal of King Saud University - Engineering Sciences*, 25(1), pp. 41–48, 2013. <https://doi.org/10.1016/j.jksues.2011.11.001>
- [33] Hanizam, H., Salleh, M. S., Omar, M. Z., Sulong, A. B. "Optimisation of mechanical stir casting parameters for fabrication of carbon nanotubes-aluminium alloy composite through Taguchi method", *Journal of Materials Research and Technology*, 8(2), pp. 2223–2231, 2019. <https://doi.org/10.1016/j.jmrt.2019.02.008>
- [34] Ramamoorthi, R., Justin Maria Hillary, J., Sundaramoorthy, R., Dixon Jim Joseph, J., Kalidas, K., Manickaraj, K. "Influence of stir casting route process parameters in fabrication of aluminium matrix composites – A review", *Materials Today: Proceedings*, 45, pp. 6660–6664, 2021. <https://doi.org/10.1016/j.matpr.2020.12.068>
- [35] ASTM "ASTM E8/E8M-24 Standard Test Methods for Tension Testing of Metallic Materials", ASTM International, West Conshohocken, PA, USA, 2024. https://doi.org/10.1520/E0008_E0008M-24
- [36] ASTM "ASTM E23-25 Standard Test Methods for Notched Bar Impact Testing of Metallic Materials", ASTM International, West Conshohocken, PA, USA, 2025. <https://doi.org/10.1520/E0023-25>
- [37] Ning, F., Chunming, Z., Zunjie, W., Hongwei, W., Xuejian, Z., Tao, C. "Effect of Ge and Mg additions on the aging response behavior and mechanical properties of Al-Si-Cu alloy", *Materials Science and Engineering: A*, 811, 141024, 2021. <https://doi.org/10.1016/j.msea.2021.141024>
- [38] Gebril, M. A., Omar, M. Z., Mohamed, I. F., Othman, N. K., Aziz, A. M., Irfan, O. M. "The Microstructural Refinement of the A356 Alloy Using Semi-Solid and Severe Plastic-Deformation Processing", *Metals*, 13(11), 1843, 2023. <https://doi.org/10.3390/met13111843>

- [39] Reisi, M., Niroumand, B. "Effects of stirring parameters on rheocast structure of Al–7.1wt.%Si alloy", *Journal of Alloys and Compounds*, 470(1–2), pp. 413–419, 2009.
<https://doi.org/10.1016/j.jallcom.2008.02.104>
- [40] Abdullah, M. E., Mohammed, M. M., Ahmed, F. S., Kubit, A., Aghajani Derazkola, H. "Evaluating the microstructural and mechanical properties of TiO₂/AA7075 metal matrix nanocomposite via friction stir processing", *The International Journal of Advanced Manufacturing Technology*, 137(9), pp. 4741–4760, 2025.
<https://doi.org/10.1007/s00170-025-15437-7>
- [41] Mathers, G., "The welding of aluminium and its alloys", Woodhead Publishing, 2002. ISBN 978-1-85573-567-5
- [42] Dieter, G. E. "Mechanical Metallurgy", McGraw-Hill Book Company (UK) Limited, 1988. ISBN 0-07-084187-X
- [43] Yang, S. "A356 Aluminum Die Casting: Best Alloy for Automotive and Aerospace", [online] Available at: <https://aludiecasting.com/a356-aluminum-die-casting/> [Accessed: 05 June 2025]